Published in final edited form as:

Nature. 2018 November ; 563(7730): 254–258. doi:10.1038/s41586-018-0662-5.

Resting zone of the growth plate harbors a unique class of skeletal stem cells

Koji Mizuhashi[1], **Wanida Ono**[1], **Yuki Matsushita**[1], **Naoko Sakagami**[1], **Akira Takahashi**[1], **Thomas L. Saunders**[2], **Takashi Nagasawa**[3], **Henry M. Kronenberg**[4], and **Noriaki Ono**[1,*]

[1]University of Michigan School of Dentistry, Ann Arbor, MI, 48109, USA

[2]Transgenic Animal Model Core, University of Michigan Medical School, Ann Arbor, MI, 48109, USA

[3]Laboratory of Stem Cell Biology and Developmental Immunology, Graduate School of Frontier Biosciences, Osaka University School of Medicine, Suita, Osaka, 565-0871, Japan

[4]Endocrine Unit, Massachusetts General Hospital and Harvard Medical School, Boston, MA, 02114, USA

Summary

Skeletal stem cells regulate bone growth and homeostasis by generating diverse cell types including chondrocytes, osteoblasts and marrow stromal cells. The emerging model postulates a distinct type of skeletal stem cells closely associated with the growth plate[1-4], a special cartilaginous tissue playing critical roles in bone elongation[5]. The resting zone maintains the growth plate by expressing parathyroid hormone-related protein (PTHrP) that interacts with Indian hedgehog (Ihh) released from the hypertrophic zone[6-10], while providing a source of other chondrocytes[11]. However, the identity of skeletal stem cells and how they are maintained in the growth plate are unknown. Here we show that skeletal stem cells are formed among PTHrP$^+$ chondrocytes within the resting zone of the postnatal growth plate. PTHrP$^+$ chondrocytes expressed a panel of markers for skeletal stem/progenitor cells and uniquely possessed the properties as skeletal stem cells in cultured conditions. Cell lineage analysis revealed that PTHrP$^+$ resting chondrocytes continued to form columnar chondrocytes long term, which underwent hypertrophy and became osteoblasts and marrow stromal cells beneath the growth plate. Transit-amplifying chondrocytes in the proliferating zone, which was concertedly maintained by a forward signal from undifferentiated cells (PTHrP) and a reverse signal from hypertrophic cells (Ihh), provided instructive cues to maintain cell fates of PTHrP$^+$ resting chondrocytes. Our findings

*Correspondence: Noriaki Ono, noriono@umich.edu.

Author contributions K.M. and N.O. conceived the project and designed the experiments; K.M. and N.O. performed the mouse genetic experiments with assistance from W.O., N.S. and A.T. who performed genotyping; K.M. performed histological experiments and imaging analysis; K.M. performed cell culture experiments; K.M. and N.O. performed flow cytometry experiments and analysis; Y.M. performed the surgery and cell transplantation; K.M. and N.O. analyzed the data; N.O. supervised the project; T.L.S. generated the mice; T.N. provided the mice; K.M. and N.O. wrote the manuscript; T.N., W.O. and H.M.K. critiqued the manuscript.

Author Information Reprints and permissions information is available at www.nature.com/reprints. The authors declare no competing financial interests. Readers are welcome to comment on the online version of the paper. Correspondence and requests for materials should be addressed to N.O. (noriono@umich.edu).

Reviewer information *Nature* thanks anonymous reviewers for the contribution to the peer review of this work.

unravel a unique somatic stem cell type that is initially unipotent and acquires multipotency at the post-mitotic stage, underscoring the malleable nature of the skeletal cell lineage. This system provides a model in which functionally dedicated stem cells and their niche are specified postnatally and maintained throughout tissue growth by a tight feedback regulation system.

We first defined the formation PTHrP^{+} chondrocytes in the growth plate using a *PTHrP*-mCherry knock-in reporter allele (Extended Data Fig.1a, see also Supplementary Information). During the fetal stage, *PTHrP*-mCherry^{+} cells were mitotically active and localized within the Sox9^{+} perichondrial region (Extended Data Fig.1b). While this pattern continued at birth (Fig.1a), a distinct group of *PTHrP*-mCherry^{+} chondrocytes appeared in the central area of the growth plate devoid of proliferation at P3 (Extended Data Fig.1c). These *PTHrP*-mCherry^{+} chondrocytes increased their number drastically between P6 and P9 and occupied a well-defined zone in the growth plate (Fig.1b-1d, Extended Data Fig.1c), and were less proliferative than their counterparts in the proliferating zone (EdU^{+}; 6.1±2.3% of mCherry^{+} cells vs. 30.5±3.2% of proliferating chondrocytes at P9, n=3 mice). Therefore, *PTHrP*-mCherry^{+} resting chondrocytes develop in the postnatal growth plate closely associated with the formation of secondary ossification centers. Flow cytometry analysis revealed that *PTHrP*-mCherry^{+} cells were exclusively found in CD45^{neg} growth plate cells (Fig.1e), while completely absent in CD45^{neg} bone/bone marrow cells (Extended Data Fig. 2a). *PTHrP*-mCherry^{+} growth plate cells did not express *Col1(2.3kb)*-GFP (Extended Data Fig.2b), indicating that *PTHrP*-mCherry is specifically expressed by growth plate chondrocytes, but not by osteoblasts or bone marrow stromal cells. We next asked whether *PTHrP*-mCherry^{+} resting chondrocytes express a panel of cell surface markers for transplantable skeletal stem/progenitor cells[3], particularly three subsets of skeletal stem/progenitor populations (AlphaV[CD51]$^{+}$Thy[CD90]$^{-}$); mouse skeletal stem cells (mSSC, CD105^{-}CD200^{+}), pre-bone/cartilage/stromal progenitor (pre-BCSP, CD105^{-}CD200^{-}) and bone/cartilage/stromal progenitor (BCSP, CD105^{+}). A great majority of CD45^{-}Ter119^{-}CD31^{-} growth plate cells, including both mCherry^{-} and mCherry^{+} fractions, were in a CD51^{+}CD90^{-} skeletal stem/progenitor population (Fig.1f, upper panels). Among CD45^{-}Ter119^{-}CD31^{-}CD51^{+}CD90^{-}mCherry^{+} cells, 49.2±8.4%, 23.4±8.4% and 27.4±16.5% were CD105^{-}CD200^{+} (mSSC), CD105^{-}CD200^{-} (pre-BCSP) and CD105^{+} (BCSP), respectively (Fig.1f, lower panels, see also Extended Data Fig.2c,2d). Conversely, 41.6±4.4%, 31.7±6.2% and 53.4±16.9% of mSSC, pre-BCSP and BCSP, respectively, were positive for *PTHrP*-mCherry (Extended Data Fig.2e). Therefore, *PTHrP*-mCherry^{+} resting chondrocytes represent a substantial subset of immunophenotypically defined skeletal stem/progenitor cells in the growth plate.

We next determined whether PTHrP^{+} resting chondrocytes behave as stem cells *in vivo* using a *PTHrP-creER* bacterial artificial chromosome (BAC) transgenic line (L909, Extended Data Fig.3a, see also Supplementary Information). Analysis of *PTHrP*$^{mCherry/+}$; *PTHrP-creER; R26R*-ZsGreen mice revealed that ZsGreen^{+} cells largely overlapped with mCherry^{+} cells shortly after a tamoxifen pulse at P6 (Extended Data Fig.3b-3d). The percentage of CD105^{+} cells within ZsGreen^{+} cells was significantly lower than that of mCherry^{+} cells (Extended Data Fig.3e), indicating that *PTHrP-creER* preferentially marks an immature subset of *PTHrP*-mCherry^{+} cells. An EdU label-exclusion assay of P6-pulsed

PTHrP-creER; *R26R*-tdTomato mice revealed that a great majority of tdTomato$^+$ cells were resistant to EdU incorporation (Extended Data Fig.3f, EdU$^+$; 7.7±2.0% of tdTomato$^+$ cells vs. 61.1±11.5% of proliferating zone chondrocytes, n=3 mice), demonstrating that *PTHrP-creER* specifically marks resting chondrocytes (Extended Data Fig.3g). These PTHrP$^+$ resting chondrocytes did not express Grem1[4] (Extended Data Fig.3h). Subsequently, we traced the fate of P6-labelled PTHrP$^+$ resting chondrocytes *in vivo* (PTHrP^{CE}-P6 cells). After remaining within the resting zone at P12 (Fig.2a, see also Extended Data Fig.3g), PTHrP^{CE}-P6 cells first formed short columns (composed of <10 cells) (Fig.2b, arrowhead), then subsequently formed longer columns (composed of >10 cells) originating from the resting zone toward P18 (Fig.2c, arrows). After a month of chase, PTHrP^{CE}-P6 cells constituted the entire column from the resting zone to the hypertrophic zone (Fig.2d). The number of tdTomato$^+$ resting chondrocytes transiently increased during the first week of chase and decreased thereafter due to the formation of columnar chondrocytes (Fig.2e). The number of short tdTomato$^+$ columns peaked at P18 and decreased thereafter, whereas long tdTomato$^+$ columns appeared at P18 and continued to increase toward P36 (Fig.2f). Thus, *PTHrP-creER*$^+$ resting chondrocytes stay within the resting zone for the first week, and establish columnar chondrocytes starting from the second week of chase. Analysis of *PTHrP-creER*; *R26R*-Confetti mice revealed that each column was marked by its unique color (CFP, YFP or tdTomato, Fig.2g), demonstrating that single *PTHrP-creER*$^+$ resting chondrocytes can give rise to multiple types of chondrocytes. Additional analysis of *Col2a1-creER*; *R26R*-Confetti mice further supported the existence of clonal cell populations (Extended Data Fig.4a). Together, these findings support the notion that individual PTHrP$^+$ resting chondrocytes are multipotent and can clonally establish columnar chondrocytes in the growth plate.

To investigate whether *PTHrP-creER*$^+$ resting chondrocytes undergo self-renewing asymmetric divisions, we performed an EdU label-retention assay. Analysis of PTHrP^{CE}-P6 cells with serial pulses of EdU revealed that, after 3 weeks of chase, these cells gradually diluted EdU signal as they differentiated toward the hypertrophic zone (Fig.2h). Further, PTHrP^{CE}-P6 cells in the resting zone expressed *PTHrP*-mCherry, while those in the proliferating zone lost its expression (Fig.2i). Therefore, *PTHrP-creER*$^+$ chondrocytes maintain themselves in the resting zone as PTHrP$^+$ cells and become the source of columnar chondrocytes in the growth plate by providing the transit-amplifying progeny. Analysis of *PTHrP-creER*; *R26R*-tdTomato mice after being pulsed at various preceding prenatal and early postnatal time points revealed that *PTHrP-creER*$^+$ chondrocytes started to be formed within the resting zone at E17.5 (Extended Data Fig.4b-4e), in which a tamoxifen pulse at a later day laterally expanded the domain of tdTomato$^+$ cells. However, once they were marked, tdTomato$^+$ cells did not expand laterally upon further chase (Extended Data Fig.4f, 4g), indicating that PTHrP$^+$ resting chondrocytes are rather dedicated to making columnar chondrocytes longitudinally. Additional analysis of *Dlx5-creER*; *R26R*-tdTomato mice revealed that chondrocytes in the proliferating and hypertrophic zone could only form short columns (<10 cells) that eventually disappeared from the growth plate (Extended Data Fig. 5a-5d), indicating that *Dlx5-creER*$^+$ proliferating chondrocytes are not the source of columnar chondrocytes in the growth plate.

During an extended chase period, PTHrP^{CE}-P6 cells continued to form columnar chondrocytes within the growth plate for at least a year after the pulse (Fig.3a-3c for *Col1(2.3kb)*-GFP, Extended Data Fig.6a-6d for *Cxcl12*-GFP[12]), in which the number of tdTomato^{+} columns gradually decreased until 6 months after the pulse and reached a plateau thereafter (Fig.3d). A majority of tdTomato^{+} columns extended beyond the hypertrophic layer and continued into the primary spongiosa and the metaphyseal bone marrow, an area beneath the growth plate[13]. These chondrocytes became *Cxcl1*2-GFP^{+} stromal cells beneath tdTomato^{+} columns (Extended Data Fig.6e) and reticular cells near trabecular bones (Fig.3a, lower panel). These chondrocytes also became *Col1(2.3kb)*-GFP^{+} osteoblasts on the trabecular surface (Fig.3a, lower panel) and in the primary spongiosa (Fig.3b, lower panel). The number of *Cxcl12*-GFP^{+}tdTomato^{+} stromal cells and *Col1a1(2.3kb)*-GFP^{+}tdTomato^{+} osteoblasts increased for the first three months of chase; subsequently, the number of *Col1a1(2.3kb)*-GFP^{+}tdTomato^{+} osteoblasts decreased, whereas the number of *Cxcl12*-GFP $^{+}$tdTomato^{+} stromal cells reached a plateau (Fig.3e). These cells did not become bone marrow adipocytes in the presence of high-fat diet containing a PPARγ agonist rosiglitazone (LipidTOX^{+}; 0/443 cells examined, Extended Data Fig.6f). Therefore, a subset of *PTHrP-creER*$^{+}$ resting chondrocytes can continue to reproduce themselves within the resting zone long term, while their descendants first differentiate into hypertrophic chondrocytes within the growth plate, then become multiple types of cells beyond the growth plate, such as osteoblasts and bone marrow stromal cells, but not adipocytes *in vivo*.

We next performed a colony-forming assay to test if *PTHrP-creER*$^{+}$ resting chondrocytes behave as skeletal stem cells in cultured conditions[14,15]. PTHrP^{CE}-P6 cells formed distinct tdTomato^{+} large colonies (>50 cells) composed of small Sox9^{+} round-shaped cells (~20μm in diameter) (Extended Data Fig.7a,7b). By contrast, Dlx5^{CE}-P7 cells failed to form tdTomato^{+} colonies (Extended Data Fig.7b, right panel), indicating that *PTHrP-creER*$^{+}$ resting chondrocytes uniquely possess the capability to form colonies when cultured *ex vivo* (Extended Data Fig.7c). We next isolated individual primary *PTHrP-creER*/tdTomato^{+} colonies and subcultured them further to determine whether individual colony-forming cells can self-renew *in vitro* (Extended Data Fig.7d, see also Supplemental Information). While a small fraction of P9 *PTHrP-creER*/tdTomato^{+} primary colonies had the ability to establish secondary colonies (17/518 clones, 3.3%), none of them could survive a further passage (Extended Data Fig.7e). By contrast, an increased fraction of P12 *PTHrP-creER*/tdTomato^{+} colonies established secondary colonies (16/98 clones, 16.3%), and a fraction of these clones (2/16 clones, 12.5%) could be further passaged at least for nine generations (Fig.4a). Thus, *PTHrP-creER*$^{+}$ colony-forming cells appear to acquire robust *in vitro* self-renewability when the secondary ossification center actively develops. Further, individual *PTHrP-creER*/ tdTomato^{+} cells (Passage 4 - 7) could generate Alcian Blue^{+} spheres, Alizarin Red^{+} mineralized matrix and LipidTOX^{+} oil droplets under chondrogenic, osteogenic and adipogenic differentiation conditions, respectively (Fig.4b, 4/4 clones, 100%). Upon subcutaneous transplantation into immunodeficient mice, these cells robustly differentiated into *Col1(2.3kb)*-GFP^{+} osteoblastic cells (Fig.4c) and effectively gave rise to Alcian Blue^{+} and Alizarin Red^{+} matrix effectively, but produced Oil red O^{+} lipid droplets only ineffectively (Extended Data Fig.7f). These findings indicate that PTHrP^{+} skeletal stem cells

are predisposed to become chondrocytes and osteoblasts *in vivo*, while possessing a baseline potential to become adipocytes in an inductive condition *in vitro*.

Lastly, we set out to investigate the functional significance of PTHrP^{+} resting chondrocytes. Inducible cell ablation experiments using *PTHrP-creER*; *Rosa26*$^{\text{lsl-tdTomato/+}}$ (Control) and *PTHrP-creER*; *Rosa26*$^{\text{lsl-tdTomato/iDTA}}$ (DTA) littermates revealed that, unexpectedly, *PTHrP-creER*$^{+}$ cells were only incompletely ablated, wherein tdTomato^{+} resting chondrocytes and columns were still observed in the DTA-induced tissue (Fig.5a,5b). Nonetheless, the height of each layer of the growth plate was altered in the DTA-induced tissue, in which the proliferating zone was significantly reduced associated with the significant expansion of the hypertrophic and the resting zone (Fig.5c). Therefore, partial loss of PTHrP^{+} cells in the resting zone is sufficient to alter the integrity of the growth plate by inducing premature hypertrophic differentiation of chondrocytes in the proliferating zone. Moreover, global manipulation of Hedgehog (Hh) signaling using Smo agonist (SAG) and antagonist (LDE-225) in P6-pulsed *PTHrP-creER*; *R26R*-tdTomato mice revealed that these regimens predominantly affected chondrocytes in the proliferating zone, without directly affecting PTHrP$^{\text{CE}}$-P6 cells in the resting zone (Extended Data Fig.8a-8c). Interestingly, both regimens resulted in a significantly reduced number of tdTomato^{+} columns (Fig.5d, see also Extended Data Fig.8d-8k), indicating that uninterrupted Hh signaling is essential to maintaining proper cell fates of PTHrP^{+} resting chondrocytes. In fact, *PTHrP-creER*$^{+}$ cells directly differentiated into *Col1(2.3kb)*-GFP^{+} osteoblasts in response to micro-perforation injury (Extended Data Fig.8l,m), indicating that PTHrP^{+} skeletal stem cells lose their physiological fate in the absence of an intact proliferating zone.

Taken together, we identified that the resting zone of the growth plate harbors a unique class of skeletal stem cells, whose transit-amplifying progeny are lineage-restricted as chondrocytes that exhibit multipotency only at the post-mitotic stage (see concluding diagram in Extended Data Fig.9a,9b). PTHrP^{+} cells are one of the stem cell subgroups organized within the resting zone, and together with other yet identified cells, these cells can concertedly contribute to long term tissue renewal. PTHrP^{+} skeletal stem cells are dedicated to making columnar chondrocytes longitudinally, and appear to derive from PTHrP^{-} cells. These PTHrP^{+} stem cells are highly hierarchical, with approximately 2 - 3% of these cells acquiring long-term self-renewability (Extended Data Fig.9b). In addition, these stem cells are endowed with the ability to maintain the integrity of the growth plate, by sending a forward signal (i.e. PTHrP) for transit-amplifying chondrocytes and maintain their proliferation and delay their hypertrophy in a non-cell autonomous manner. Therefore, PTHrP^{+} stem cells can also provide the niche for transit-amplifying cells, compatible with a model proposed in the epithelium[16]. Conversely, transit-amplifying cells, which are maintained in a Hedgehog-responsive manner, appear to provide instructive cues to determine cell fates of PTHrP^{+} stem cells within the growth plate, implicating a reciprocal interaction between the stem cells and their progeny. We assume that PTHrP^{-} short-term precursors are the principal driver for extensive bone growth occurring during postnatal development, reminiscent of a model proposed for HSCs[17,18]. It is possible that PTHrP^{+} skeletal stem cells are mainly involved in the long-term maintenance of skeletal integrity, although further details need to be clarified.

Extended Data

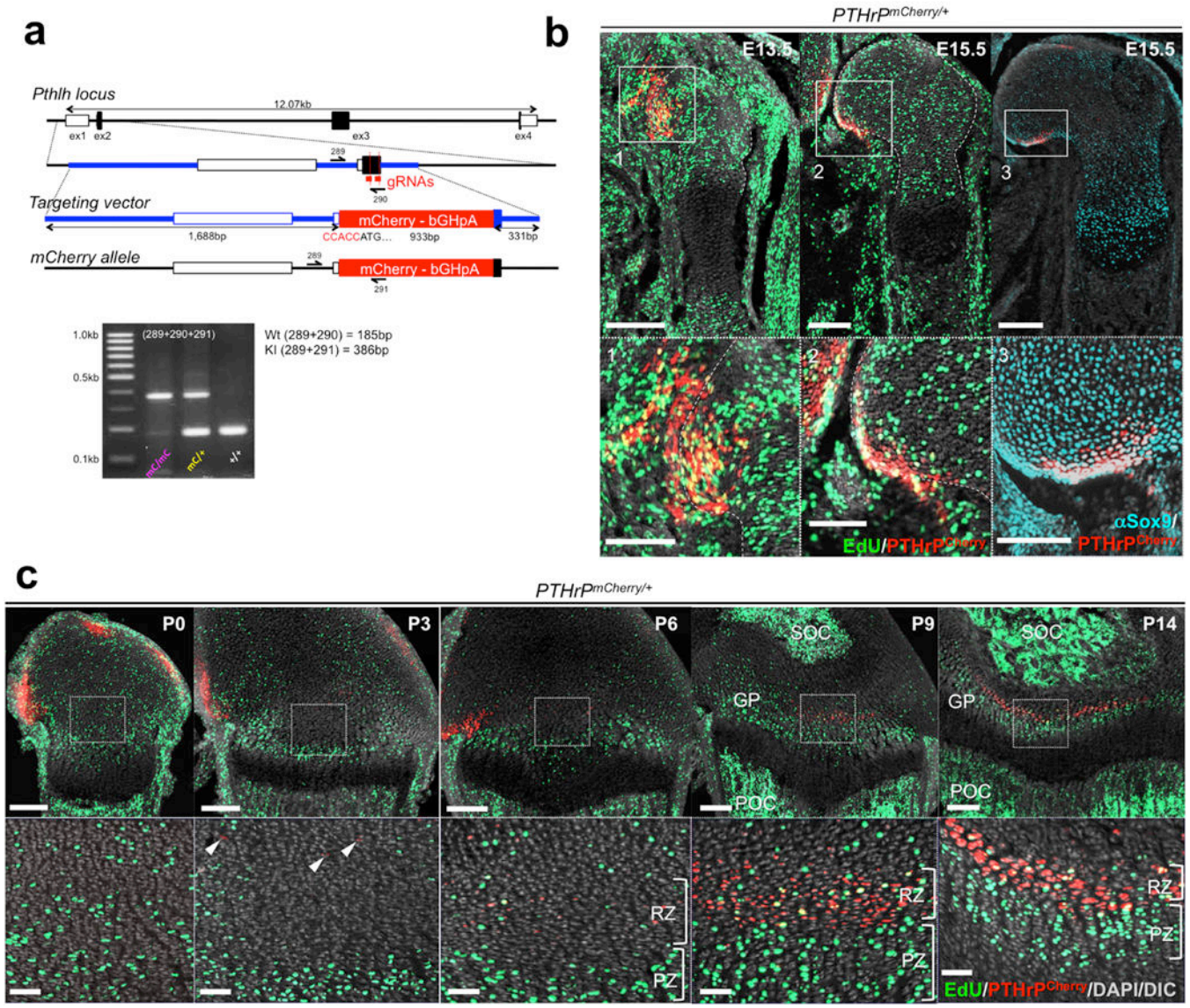

Extended Data Figure 1. Generation and characterization of *PTHrP*^{mCherry} knock-in allele.

(a) CRISP/Cas9 generation of *PTHrP*-mCherry knock-in allele. Structure of the genomic *PTHrP* locus, targeting vector and knock-in allele after homologous recombination. White boxes: untranslated region (UTR), black boxes: coding region, ex: exon. Blue bars: homology arms, red bars: guide RNAs (gRNAs) as part of CRISP/Cas6 forward (289), wild-type reverse (290) and mutant reverse (291). Lower panel: PCR genotyping using 289/290/291 primer mix, wild-type (Wt) allele: 185bp, knock-in (KI) allele: 385bp. At least n=100 independent experiments with similar results. **(b)** *PTHrP*$^{mCherry/+}$ fetal distal femurs with EdU administration shortly before analysis (3 hours). Lower panels: magnified views of perichondrium. Dotted lines: borders of bone anlage. Grey: DAPI and DIC. Scale bars: 200μm (upper panels), 100μm (lower panels). n=2 (E13.5, E15.5) mice, n=1 (αSox9) mouse. **(c)** *PTHrP*$^{mCherry/+}$ distal femur growth plates with EdU administration shortly

before analysis (3 hours). Lower panels: magnified views of central growth plates. Arrowheads: mCherry^{+} cells. RZ: resting zone, PZ: proliferating zone, GP: growth plate, POC: primary ossification center, SOC: secondary ossification center. Grey: DAPI and DIC. Scale bars: 200μm (upper panels), 50μm (lower panels).

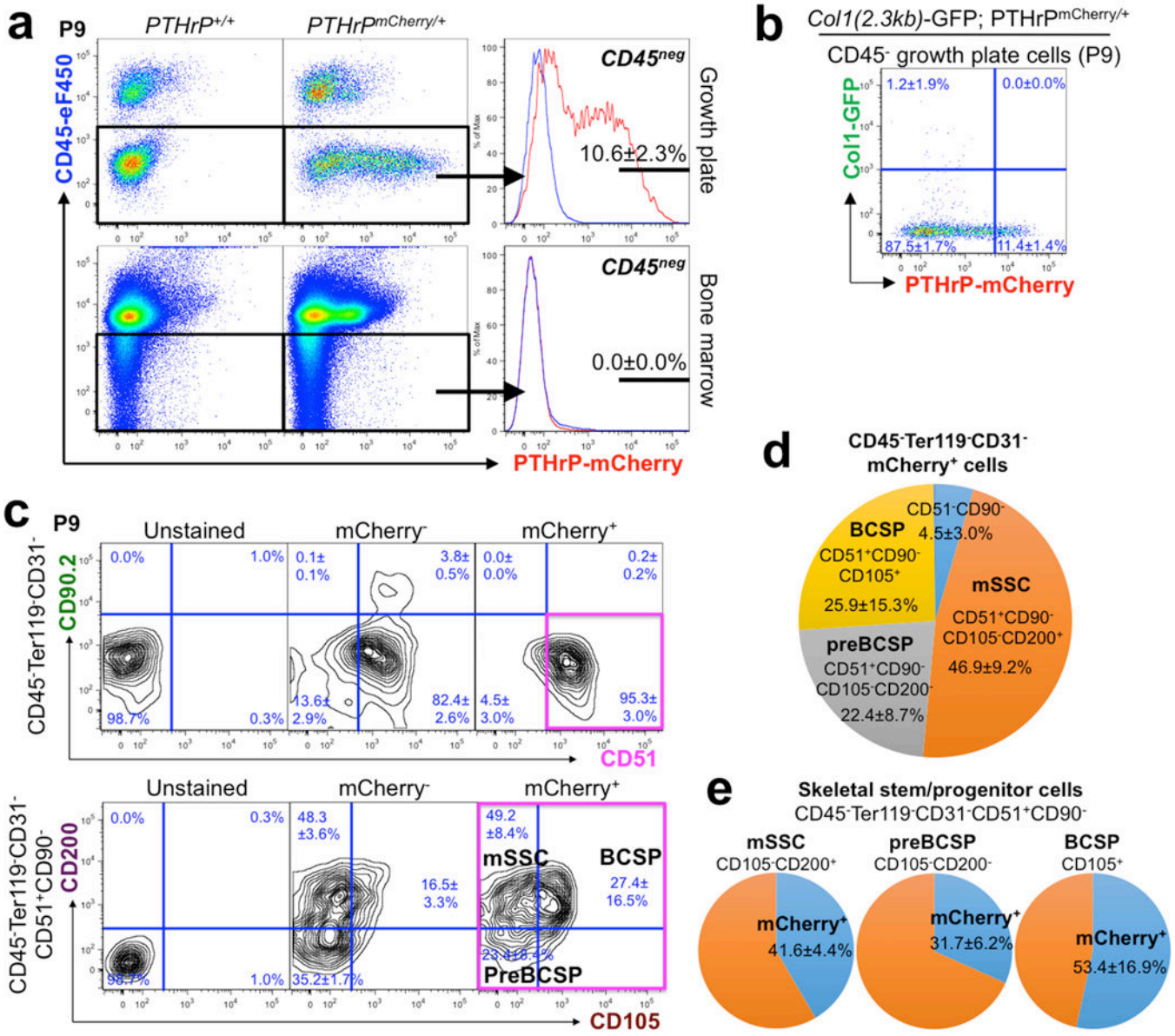

Extended Data Figure 2. Skeletal stem/progenitor cell marker expression in *PTHrP-mCherry*$^{+}$ resting chondrocytes.

(a) Flow cytometry analysis of *PTHrP*$^{mCherry/+}$ growth plate cells (upper panels) and bone marrow cells (lower panels). *n*=8 mice for *PTHrP*$^{mCherry/+}$ and *n*=3 mice for *PTHrP*$^{+/+}$, data are presented as mean ± S.D. **(b)** Flow cytometry analysis of *Col1(2.3kb)*-GFP; *PTHrP*$^{mCherry/+}$ growth plate cells. *n*=5 mice per group, data are presented as mean ± S.D. **(c)** Skeletal stem/progenitor cell surface marker analysis of *PTHrP*$^{mCherry/+}$ growth plate cells. Unstained: *PTHrP*$^{+/+}$ cells mice only stained for CD45/Ter119/CD31, mCherry^{-}:

mCherry^{-} fraction of *PTHrP*$^{mCherry/+}$ cells, mCherry^{+}: mCherry^{+} fraction of *PTHrP*$^{mCherry/+}$ cells. Magenta box: CD45^{-}Ter119^{-}CD31^{-}CD51^{+}CD90^{-}mCherry^{+} fraction. mSSC: mouse skeletal stem cell, BCSP: bone/cartilage/stromal progenitor. *n*=3 mice for *PTHrP*$^{mCherry/+}$, data are presented as mean ± S.D., *n*=1 mouse for *PTHrP*$^{+/+}$.**(d)** Composition of CD45^{-}Ter119^{-}CD31^{-}mCherry^{+} growth plate cells. mSSC: 'mouse skeletal stem cell', BCSP: 'bone/cartilage/stromal progenitor'. *n*=3 mice per group, data are presented as mean ± S.D.**(e)** Percentage of mCherry^{+} cells among mSSC (left, CD105^{-}CD200^{+}), preBCSP (left, CD105^{-}CD200^{-}) and BCSP (right, CD105^{+}), gated under CD45^{-}Ter119^{-}CD31^{-}CD51^{+}CD90^{-} fraction. mSSC: mouse skeletal stem cell, BCSP: bone/cartilage/stromal progenitor. *n*=3 mice per group, data are presented as mean ± S.D.

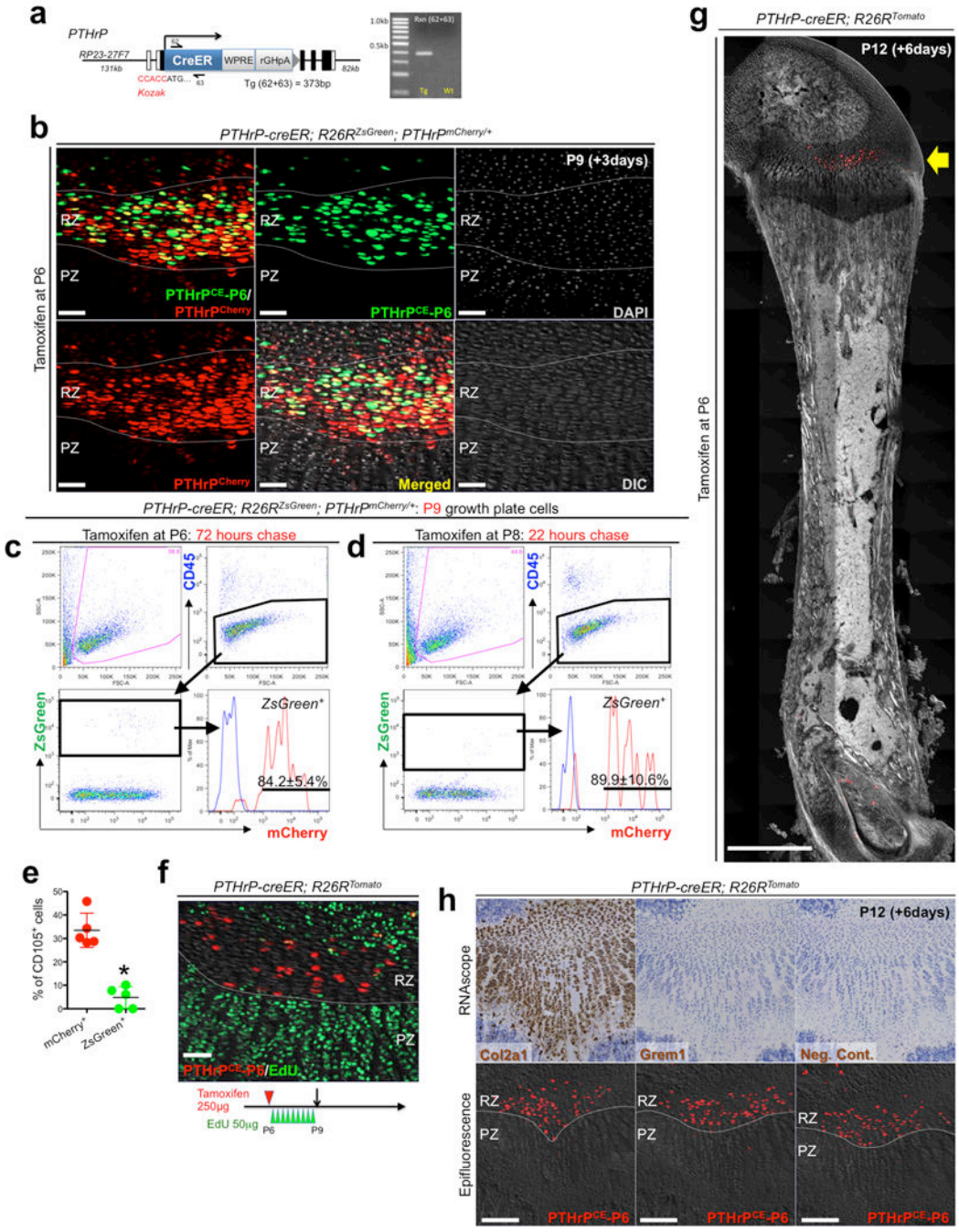

Extended Data Figure 3. Generation and characterization of *PTHrP-creER* BAC transgenic line.

(a) Generation of *PTHrP-creER* bacterial artificial chromosome (BAC) transgenic mice. Structure of the *PTHrP-creER-WPRE-rGHpA* BAC construct. *Kozak-PTHrP-creER-WPRE-rGHpA-frt-Neo^R-frt* cassette containing 62bp homology arms was recombineered into BAC clone RP23-27F7 containing 131kb upstream and 82kb downstream genomic sequences of the *PTHrP* gene. *Neo^R* and backbone *lox* sites were removed prior to pronuclear injection. Half arrows: primers, forward (62) and reverse (63). Right panel: PCR genotyping using 62/63 primer mix, transgenic (Tg): 373bp. White boxes: exons, black boxes: introns. At least

n=100 independent experiments with similar results. **(b)** Short-chase analysis of *PTHrP-creER*; *R26R*^{ZsGreen}; *PTHrP*$^{mCherry/+}$ distal femur growth plates (P6-pulsed). RZ: resting zone, PZ: proliferating zone. Scale bars: 50μm. *n*=3 mice. **(c-e)** Short-chase flow cytometry analysis of *PTHrP-creER*; *R26R*^{ZsGreen}; *PTHrP*$^{mCherry/+}$ growth plate cells, with tamoxifen injection at 72 hours (c,e) or 22 hours (d) in advance. Red lines: ZsGreen^{+} cells, Blue lines: control cells without *PTHrP*-mCherry. *n*=5 mice (72 hours) or *n*=3 mice (22 hours) per group. (e): percentage of CD105^{+} cells within mCherry^{+} (red dots) and ZsGreen^{+} (green dots) cells. *n*=5 mice per group, data are presented as mean ± S.D., **p* = 0.012, Mann-Whitney's *U*-test, two-tailed. **(f)** *PTHrP-creER*; *R26R*^{Tomato} distal femur growth plates (P6-pulsed) at P9. EdU (50μg) was serially injected 9 times at an 8-hour interval between P6 and P9. Grey: DIC. Scale bars: 50μm. *n*=3 mice. **(g)** Scanning of *PTHrP-creER*; *R26R*^{Tomato} whole femur at P12 (P6-pulsed). Arrow: tdTomato^{+} cells localized within the resting zone of distal femur. Grey: DAPI and DIC. Scale bars: 1mm. *n*=3 mice. **(h)** High sensitivity *in situ* hybridization (RNAscope) analysis of *PTHrP-creER*; *R26R*^{Tomato} distal femur growth plates at P12 (P6-pulsed). Upper and lower panels represent the identical section. Before (lower panels) and after (upper panels) hybridization. Left panels: *Col2a1* (positive control), center panels: *Grem1*, right panels: negative control. Grey: DAPI and DIC. Scale bars: 200μm. *n*=3 independent experiments.

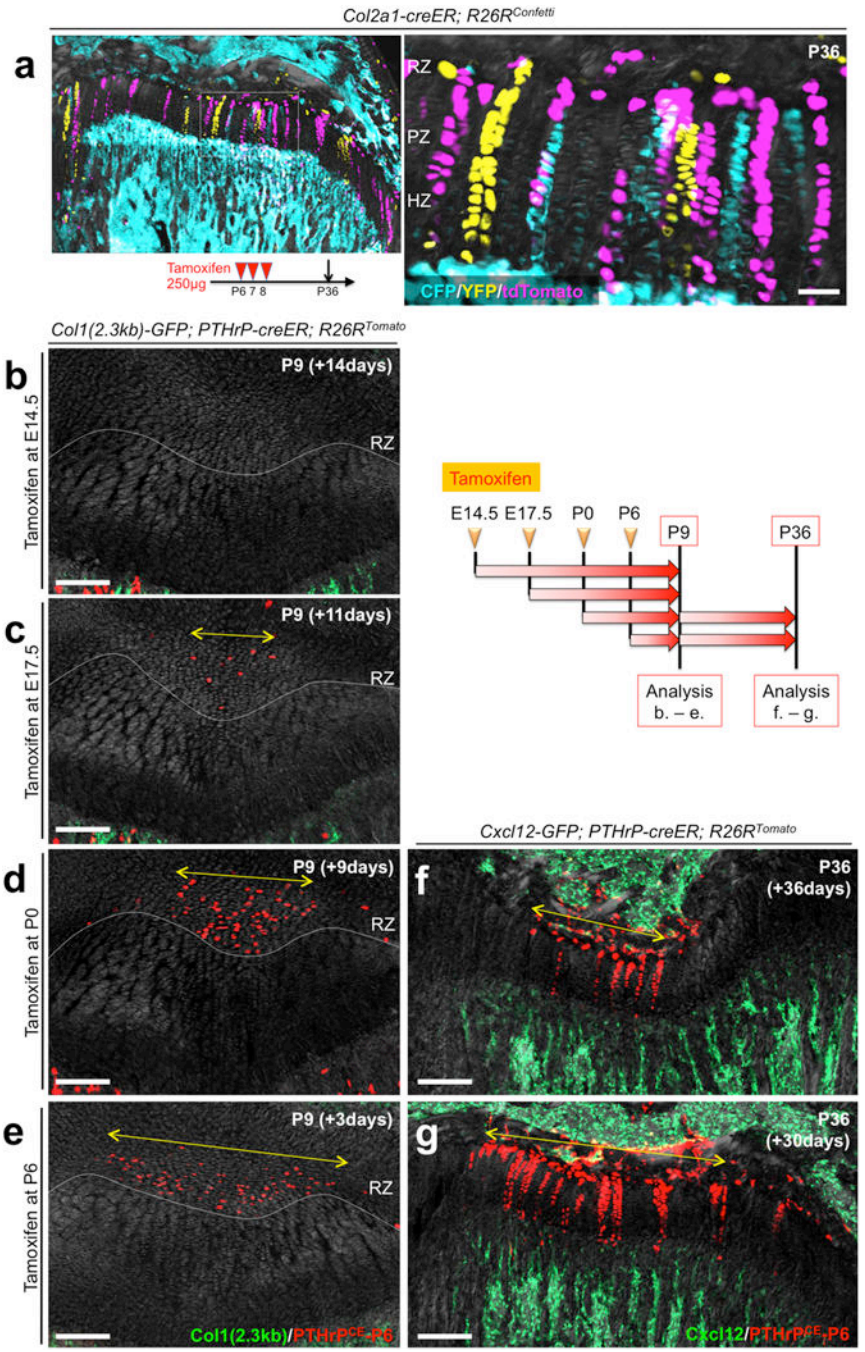

Extended Data Figure 4. PTHrP^{+} resting chondrocytes are functionally dedicated to columnar chondrocyte formation.

(a) *In vivo* clonal analysis of *Col2a1-creER*$^{+}$ growth plate chondrocytes. *Col2a1-creER; R26R*$^{\text{Confetti}}$ distal femur growth plates (P6/7/8-pulsed). RZ: resting zone, PZ: proliferating zone, HZ: hypertrophic zone. Scale bars: 50μm. *n*=2 mice.**(b-e)** *Col1(2.3kb)*-GFP; *PTHrP-creER*; *R26R*$^{\text{Tomato}}$ distal femur growth plates, P9 after being pulsed at various preceding time points. RZ: resting zone. Yellow double arrows: tdTomato^{+} domain within RZ. Grey: DAPI and DIC. Scale bars: 200μm. *n*=3 mice per group. **(f,g)** *Cxcl12*-GFP; *PTHrP-creER*;

R26R^{Tomato} distal femur growth plates, P36 after being pulsed at P0 (f) and P6 (g). Yellow double arrows in (f,g) indicate the same width as shown in (d,e). Grey: DAPI and DIC. Scale bars: 200μm. *n*=3 mice per group.

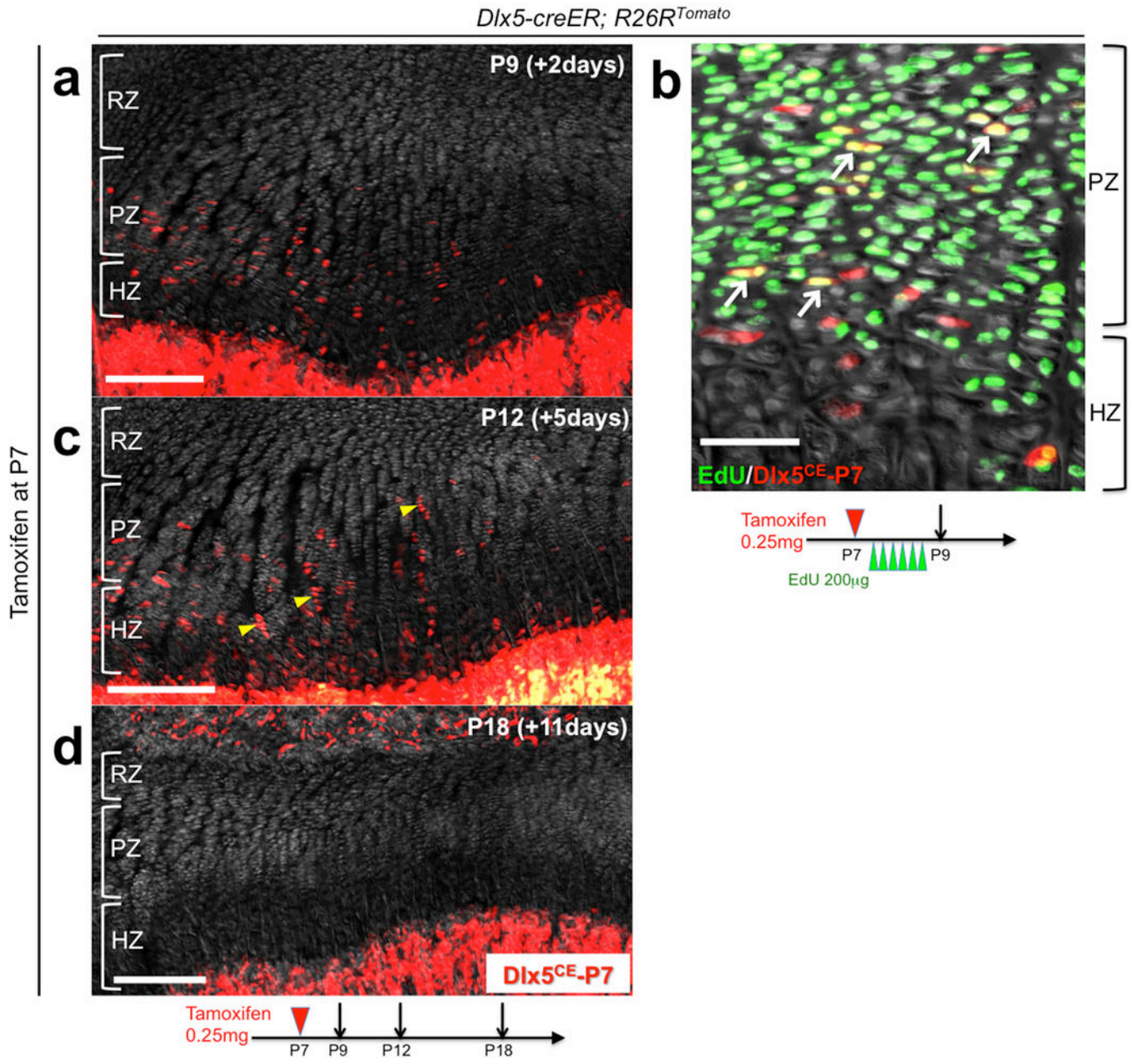

Extended Data Figure 5. *Dlx5-creER*$^{+}$ proliferating chondrocytes are not the source of columnar chondrocytes.

(a-d) Cell fate analysis of *Dlx5-creER*$^{+}$ proliferating chondrocytes. *Dlx5-creER*; *R26R*^{Tomato} distal femur growth plates (P7-pulsed). (b): EdU (200μg) was serially injected 6 times at an 8-hour interval between P7 and P9. Arrows: EdU^{+}tdTomato^{+} cells, arrowheads: short columns (<10 cells). RZ: resting zone, PZ: proliferating zone, HZ: hypertrophic zone.

Grey: DAPI and DIC. Scale bars: 200μm (left panels), 50μm (right panel). n=3 mice at each time point.

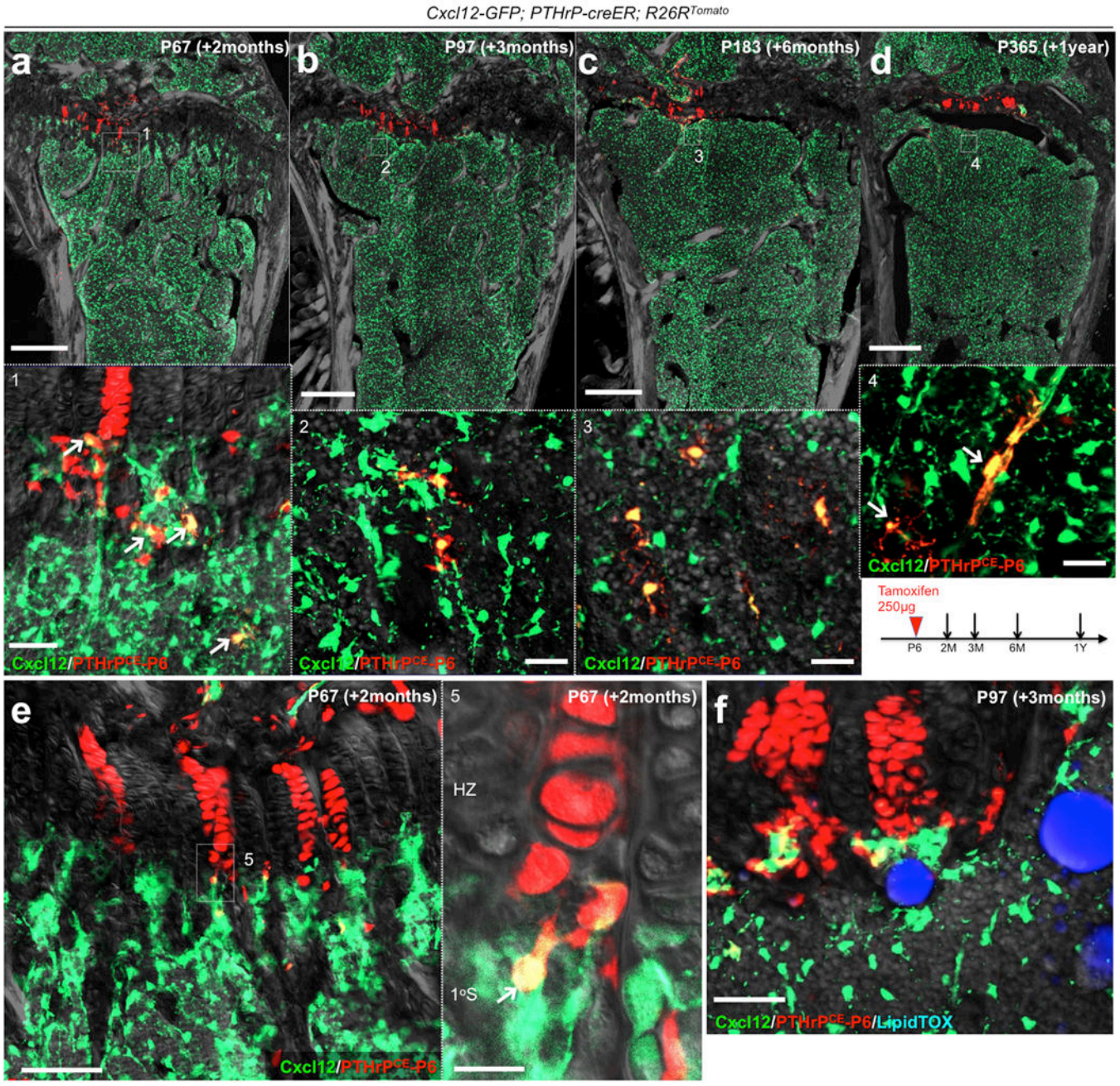

Extended Data Figure 6. PTHrP-creER$^+$ resting chondrocytes are precursors for bone marrow reticular stromal cells.

Cxcl12-GFP; *PTHrP-creER*; *R26R*^{Tomato} distal femurs (P6-pulsed). (a-d): Lower panels: magnified views of the dotted areas beneath growth plates. Arrows: *Cxcl12*-GFP$^+$tdTomato$^+$ reticular stromal cells. (e): Magnified view of the junction between hypertrophic layer and primary spongisa. Arrow: *Cxcl12*-GFP$^+$tdTomato$^+$ reticular stromal cells immediately below the hypertrophic zone. HZ: hypertrophic zone, 1^{o}S: primary spongiosa. (f): Magnified view

of the metaphyseal bone marrow. Mice were fed with high-fat diet containing rosiglitazone between P56 and P97. Grey: DAPI and DIC. Scale bars: 500μm (a-d,f), 100μm (e), 50μm (panels #1-3), 20μm (panels #4,5). *n*=3 mice for each group, except *n*=2 mice for P365.

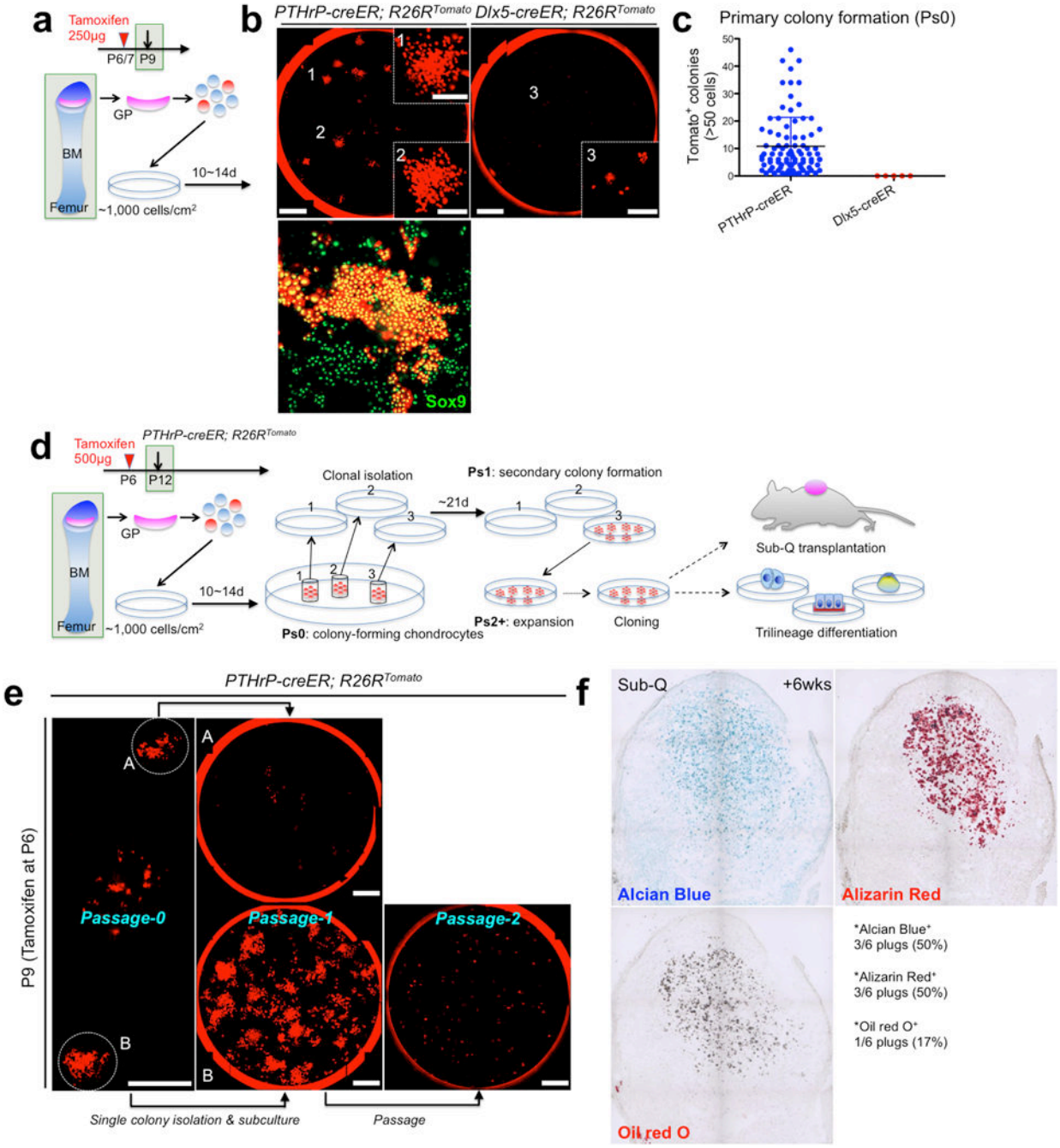

Extended Data Figure 7. *PTHrP-creER*$^+$ resting chondrocytes uniquely possess colony-forming capabilities *ex vivo*.

(a) Diagram of colony-forming assay. Growth plate cells were isolated from *PTHrP-creER*; *R26R*^{Tomato} (P6-pulsed) or *Dlx5-creER*; *R26R*^{Tomato} (P7-pulsed) mice at P9 and cultured at a clonal density (~1,000 cells/cm^2) for 10~14 days to initiate colony formation. GP: growth

plate, BM: bone marrow. **(b)** Colony-forming assay. Left panel: *PTHrP-creER*; *R26R*^{Tomato}, right panel: *Dlx5-creER*; *R26R*^{Tomato}. Insets (1,2,3): magnified views of the areas (1,2,3). Lower panel: Sox9 staining of primary *PTHrP-creER*/tdTomato^{+} colonies. Red: tdTomato. Scale bars: 5mm, 1mm (inset), 200μm (lower panel). n=88 mice for *PTHrP-creER*; *R26R*^{Tomato}, n=5 for *Dlx5-creER*; *R26R*^{Tomato}. **(c)** Quantification of tdTomato^{+} colonies (>50 cells) established from *PTHrP-creER*; *R26R*^{Tomato} (n=88) and *Dlx5-creER*; *R26R*^{Tomato} (n=5) mice. Data are presented as mean ± S.D. **(d)** Diagram of colony-forming assay and subsequent analyses on self-renewal, trilineage differentiation and transplantation of individual colony-forming cells. GP: growth plate, BM: bone marrow. **(e)** Isolation of single *PTHrP-creER*/tdTomato^{+} colonies and subsequent subculture of isolated clones. A: exhausting clone, B: self-renewing clone establishing secondary colonies. Right panel: Clone B did not proliferate at Passage 2 upon bulk culture. Red: tdTomato. Scale bars: 5mm. n=518 independent experiments **(f)** Subcutaneous transplantation of *PTHrP-creER*/tdTomato^{+} clones into immunodeficient mice. n=8 mice.

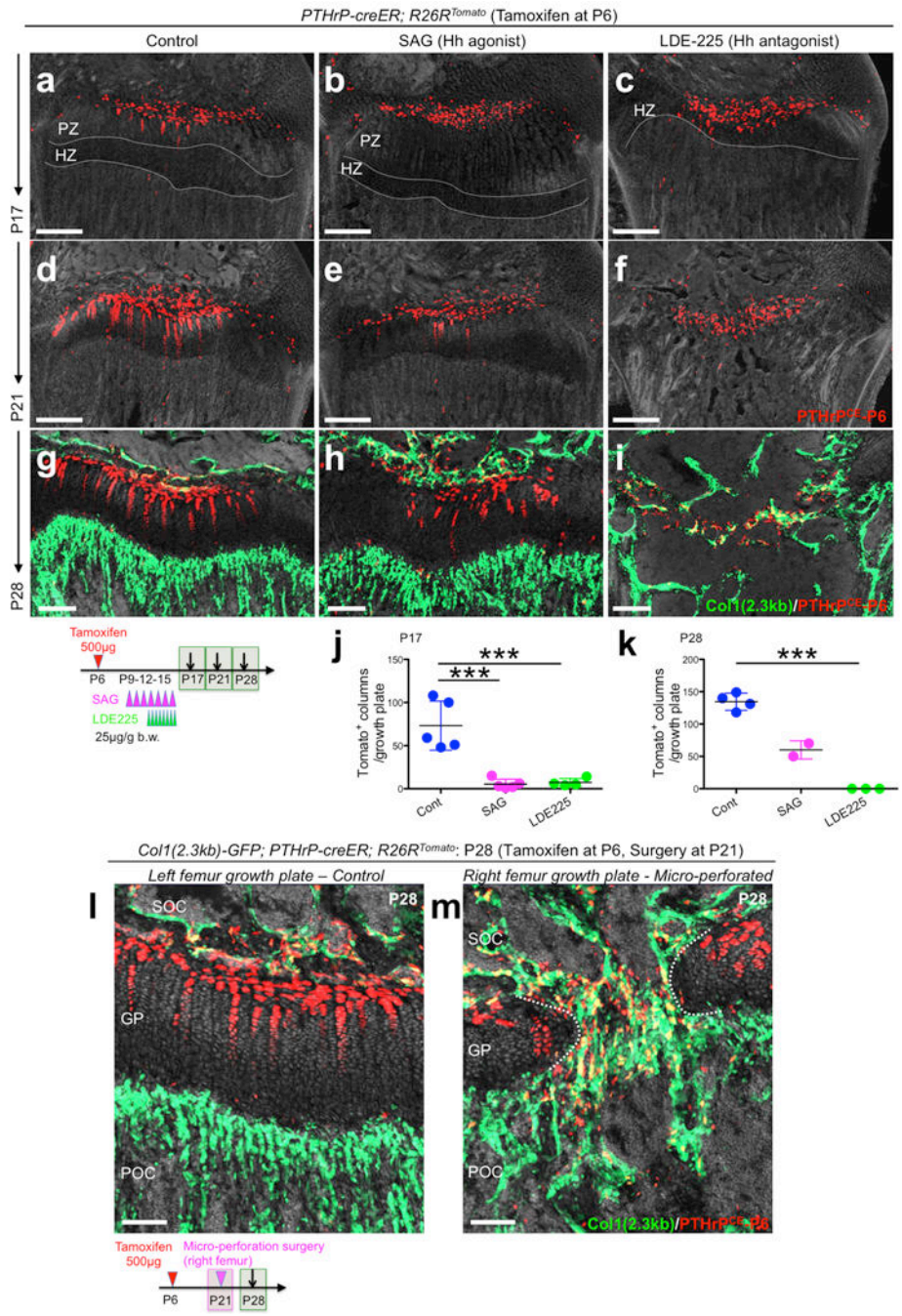

Extended Data Figure 8. *PTHrP-creER*$^{+}$ resting chondrocytes form columnar chondrocytes in a Hedgehog-responsive niche-dependent manner.

(a-i) Pharmacological manipulation of Hedgehog signaling. *PTHrP-creER*; *R26R*$^{\text{Tomato}}$ distal femur growth plates (P6-pulsed). Left panels: vehicle control, center panels: SAG (Hh agonist)-treated, right panels: LDE-225 (Hh antagonist)-treated samples. Grey: DAPI and DIC. Scale bars: 200μm. PZ: proliferating zone, HZ: hypertrophic zone. **(j,k)** Quantification of tdTomato^{+} columns in *PTHrP-creER*; *R26R*$^{\text{Tomato}}$ distal femur growth plates (P6-pulsed). P17: n=5 (Cont), n=5 (SAG), n=4 (LDE225) mice per group. P28: n=4 (Cont), n=3

(LDE225) mice per group, Data are presented as mean ± S.D. P28: n=2 (SAG). ***p < 0.001, P17 Cont vs. SAG: mean diff. = 67.8, 95% confidence interval [37.5, 98.1], P17 Cont vs. LDE225: mean diff. 66.0, 95% confidence interval [33.9, 98.0], P17 SAG vs. LDE225: mean diff. −1.85, 95% confidence interval [−33.9, 30.2], P28 Cont vs. LDE225: mean diff. 134.5, 95% confidence interval [108.7, 160.3]. One-way ANOVA followed by Tukey's multiple comparison test. **(l,m)** Mirco-perforation injury of growth plates. *Col1(2.3kb)*-GFP; *PTHrP-creER*; *R26R*^{Tomato} distal femurs (P6-pulsed) at P28. Micro-perforation surgery was performed at P21. (l): left femur growth plate (control), (m): right femur growth plate (micro-perforated). Dotted line: micro-perforated area. SOC: secondary ossification center, GP: growth plate, POC: primary ossification center. grey: DAPI and DIC. Scale bars: 100μm. n=3 mice.

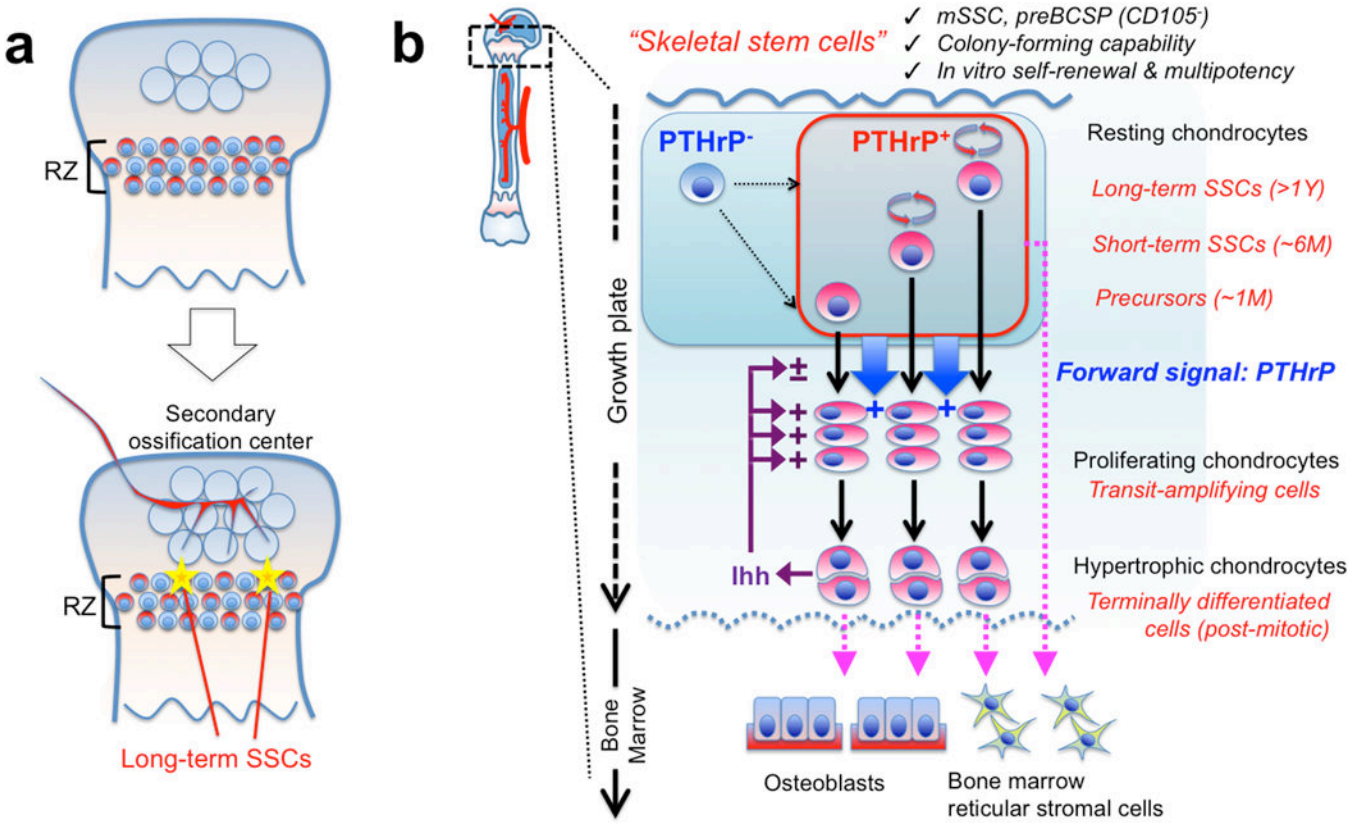

Extended Data Figure 9. Resting zone of the growth plate harbors a unique class of skeletal stem cells.

(a) Formation of PTHrP$^+$ skeletal stem cells within the growth plate. A small subset of PTHrP$^+$ chondrocytes in RZ acquire properties as long-term skeletal stem cells (SSCs) in conjunction with the formation of the highly vascularized secondary ossification center.**(b)** Concluding diagram. PTHrP$^+$ skeletal stem cells are heterogeneously composed of long-term, short-term and transient populations, and undergo asymmetric divisions and maintain themselves within RZ. These cells may be supplemented by PTHrP$^-$ cells. PTHrP$^+$ cells exert two different functions: (1) These cells differentiate into proliferating chondrocytes, hypertrophic chondrocytes and eventually become osteoblasts and bone marrow stromal

cells at the post-mitotic stage. (2) These cells send a forward signal (i.e. PTHrP) to control chondrocyte proliferation and differentiation. Indian hedgehog (Ihh) secreted by hypertrophic chondrocytes maintain proliferation of chondrocytes and formation of columnar chondrocytes. mSSC: mouse skeletal stem cell, BCSP: bone/cartilage/stromal progenitor.

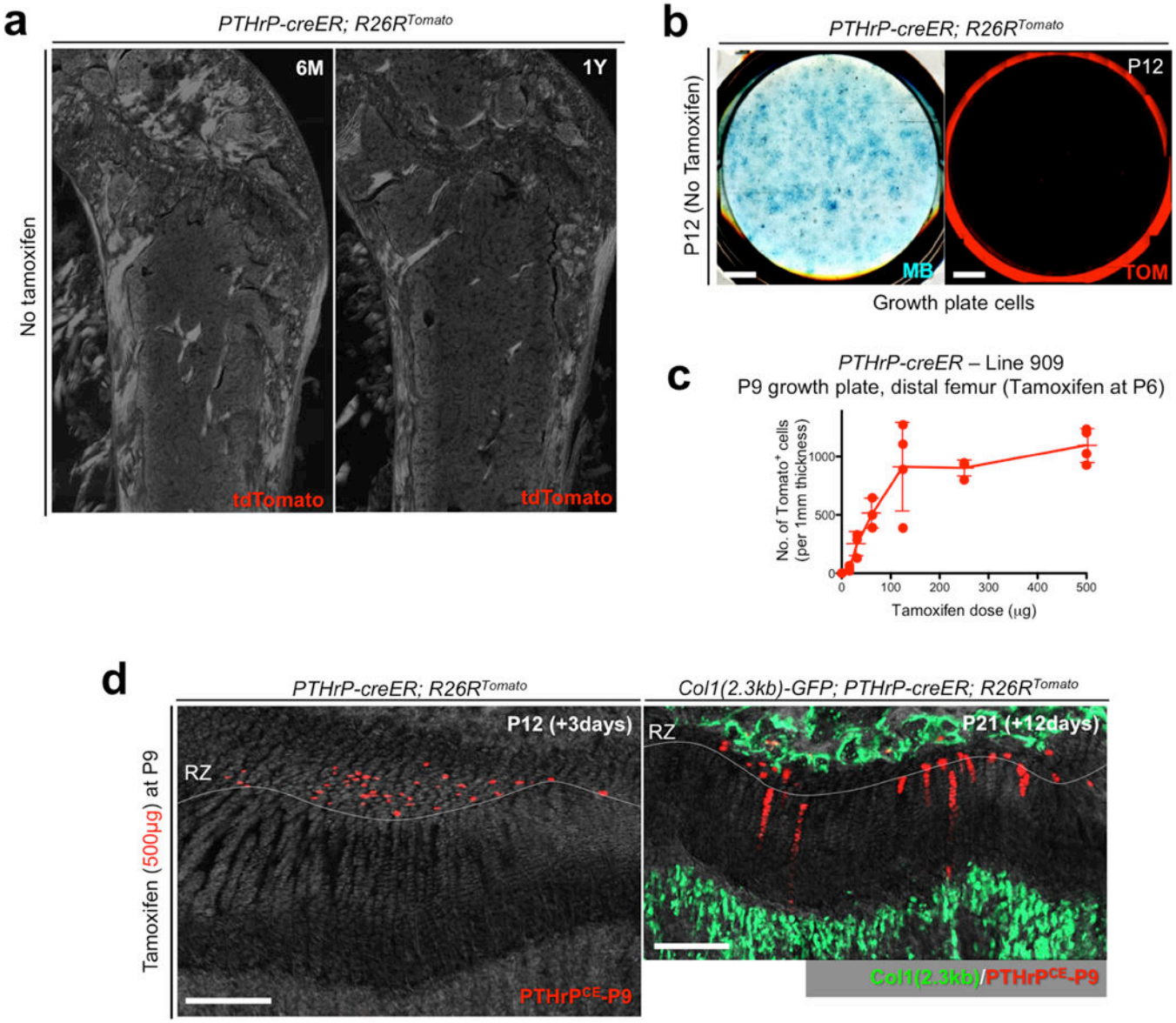

Extended Data Figure 10. Absence of tamoxifen-independent recombination in *PTHrP-creER* line.

(a) No tamoxifen controls of *PTHrP-creER*; *R26R*^{Tomato} mice at 6 months (left) and 1 year (right) of age. Red: tdTomato, blue: DAPI, grey: DIC. Scale bars: 500μm. n=3 mice per group.**(b)** No tamoxifen controls of primary colonies (Passage 0) isolated from *PTHrP-creER*; *R26R*^{Tomato} mice at P12 without tamoxifen injection. Left panel: Methylene Blue (MB) staining, right panel: red: tdTomato (TOM). Scale bar: 5mm. n=3 mice. **(c)** Dose-

response curve of *PTHrP-creER*-based recombination. Quantification of tdTomato^{+} cells in resting zone at P9 in *PTHrP-creER* (Line909); *R26R*^{Tomato} mice upon a single dose of tamoxifen at P6. *x* axis: dose of tamoxifen (μg), *y* axis: the number of tdTomato^{+} cells per 1 mm thickness. *n*=3 (0, 31.3, 62.5μg), n=4 (15.6, 125, 250, 500μg) mice per group, data are presented as mean ± S.D. **(d)** Tamoxifen-induced recombination in P9-pulsed growth plates. *PTHrP-creER*; *R26R*^{Tomato} distal femur growth plates at P12 (left) and *Col1(2.3kb)*-GFP; *PTHrP-creER*; *R26R*^{Tomato} mice at P21 (right). Tamoxifen (500μg) was injected at P9. RZ: resting zone. Green: *Col1(2.3kb)*-GFP, red: tdTomato, grey: DAPI and DIC. Scale bars: 200μm. *n*=3 mice.

Supplementary Material

Refer to Web version on PubMed Central for supplementary material.

Acknowledgements

We thank D. Holcomb and M. Curtis of Carl Zeiss Microscopy for assistance in imaging, G. Gavrilina and W. Fillipak of University of Michigan Transgenic Animal Model Core for assistance in transgenesis. This research was supported by NIH R01DE026666 and R00DE022564 (to N.O.), R03DE027421 (to W.O.), P01DK011794 (to H.M.K.), 2017 Fred F. Schudy Memorial Research Award from the American Association of Orthodontists Foundation (to N.O.) and University of Michigan MCubed 2.0 Grant (to N.O. and W.O.).

References

1. Ono N & Kronenberg HM Bone repair and stem cells. Curr Opin Genet Dev 40, 103–107, doi: 10.1016/j.gde.2016.06.012 (2016). [PubMed: 27399886]
2. Ono N, Ono W, Nagasawa T & Kronenberg HM A subset of chondrogenic cells provides early mesenchymal progenitors in growing bones. Nat Cell Biol 16, 1157–1167, doi:10.1038/ncb3067 (2014). [PubMed: 25419849]
3. Chan CK et al. Identification and specification of the mouse skeletal stem cell. Cell 160, 285–298, doi:10.1016/j.cell.2014.12.002 (2015). [PubMed: 25594184]
4. Worthley DL et al. Gremlin 1 identifies a skeletal stem cell with bone, cartilage, and reticular stromal potential. Cell 160, 269–284, doi:10.1016/j.cell.2014.11.042 (2015). [PubMed: 25594183]
5. Kronenberg HM Developmental regulation of the growth plate. Nature 423, 332–336, doi:10.1038/nature01657 (2003). [PubMed: 12748651]
6. St-Jacques B, Hammerschmidt M & McMahon AP Indian hedgehog signaling regulates proliferation and differentiation of chondrocytes and is essential for bone formation. Genes Dev 13, 2072–2086 (1999). [PubMed: 10465785]
7. Kobayashi T et al. PTHrP and Indian hedgehog control differentiation of growth plate chondrocytes at multiple steps. Development 129, 2977–2986 (2002). [PubMed: 12050144]
8. Kobayashi T et al. Indian hedgehog stimulates periarticular chondrocyte differentiation to regulate growth plate length independently of PTHrP. J Clin Invest 115, 1734–1742, doi:10.1172/JCI24397 (2005). [PubMed: 15951842]
9. Chen X et al. Initial characterization of PTH-related protein gene-driven lacZ expression in the mouse. J Bone Miner Res 21, 113–123, doi:10.1359/JBMR.051005 (2006). [PubMed: 16355280]
10. Mak KK, Kronenberg HM, Chuang PT, Mackem S & Yang Y Indian hedgehog signals independently of PTHrP to promote chondrocyte hypertrophy. Development 135, 1947–1956, doi: 10.1242/dev.018044 (2008). [PubMed: 18434416]
11. Abad V et al. The role of the resting zone in growth plate chondrogenesis. Endocrinology 143, 1851–1857, doi:10.1210/endo.143.5.8776 (2002). [PubMed: 11956168]

12. Ara T et al. A role of CXC chemokine ligand 12/stromal cell-derived factor-1/pre-B cell growth stimulating factor and its receptor CXCR4 in fetal and adult T cell development in vivo. J Immunol 170, 4649–4655 (2003). [PubMed: 12707343]
13. Yang L, Tsang KY, Tang HC, Chan D & Cheah KS Hypertrophic chondrocytes can become osteoblasts and osteocytes in endochondral bone formation. Proc Natl Acad Sci U S A 111, 12097–12102, doi:10.1073/pnas.1302703111 (2014). [PubMed: 25092332]
14. Bianco P et al. The meaning, the sense and the significance: translating the science of mesenchymal stem cells into medicine. Nat Med 19, 35–42, doi:10.1038/nm.3028 (2013). [PubMed: 23296015]
15. Bianco P "Mesenchymal" stem cells. Annu Rev Cell Dev Biol 30, 677–704, doi:10.1146/annurev-cellbio-100913-013132 (2014). [PubMed: 25150008]
16. Pardo-Saganta A et al. Parent stem cells can serve as niches for their daughter cells. Nature 523, 597–601, doi:10.1038/nature14553 (2015). [PubMed: 26147083]
17. Sun J et al. Clonal dynamics of native haematopoiesis. Nature 514, 322–327, doi:10.1038/nature13824 (2014). [PubMed: 25296256]
18. Busch K et al. Fundamental properties of unperturbed haematopoiesis from stem cells in vivo. Nature 518, 542–546, doi:10.1038/nature14242 (2015). [PubMed: 25686605]
19. Cong L et al. Multiplex genome engineering using CRISPR/Cas systems. Science 339, 819–823, doi:10.1126/science.1231143 (2013). [PubMed: 23287718]
20. Mali P et al. RNA-guided human genome engineering via Cas9. Science 339, 823–826, doi:10.1126/science.1232033 (2013). [PubMed: 23287722]
21. Hsu PD et al. DNA targeting specificity of RNA-guided Cas9 nucleases. Nat Biotechnol 31, 827–832, doi:10.1038/nbt.2647 (2013). [PubMed: 23873081]
22. Ran FA et al. Genome engineering using the CRISPR-Cas9 system. Nat Protoc 8, 2281–2308, doi:10.1038/nprot.2013.143 (2013). [PubMed: 24157548]
23. Pettitt SJ et al. Agouti C57BL/6N embryonic stem cells for mouse genetic resources. Nat Methods 6, 493–495, doi:10.1038/nmeth.1342 (2009). [PubMed: 19525957]
24. Sakurai T, Watanabe S, Kamiyoshi A, Sato M & Shindo T A single blastocyst assay optimized for detecting CRISPR/Cas9 system-induced indel mutations in mice. BMC Biotechnol 14, 69, doi:10.1186/1472-6750-14-69 (2014). [PubMed: 25042988]
25. Goodwin EC & Rottman FM The 3'-flanking sequence of the bovine growth hormone gene contains novel elements required for efficient and accurate polyadenylation. J Biol Chem 267, 16330–16334 (1992). [PubMed: 1644817]
26. Van Keuren ML, Gavrilina GB, Filipiak WE, Zeidler MG & Saunders TL Generating transgenic mice from bacterial artificial chromosomes: transgenesis efficiency, integration and expression outcomes. Transgenic Res 18, 769–785, doi:10.1007/s11248-009-9271-2 (2009). [PubMed: 19396621]
27. Kalajzic I et al. Use of type I collagen green fluorescent protein transgenes to identify subpopulations of cells at different stages of the osteoblast lineage. J Bone Miner Res 17, 15–25, doi:10.1359/jbmr.2002.17.1.15 (2002). [PubMed: 11771662]
28. Taniguchi H et al. A resource of Cre driver lines for genetic targeting of GABAergic neurons in cerebral cortex. Neuron 71, 995–1013, doi:10.1016/j.neuron.2011.07.026 (2011). [PubMed: 21943598]
29. Nakamura E, Nguyen MT & Mackem S Kinetics of tamoxifen-regulated Cre activity in mice using a cartilage-specific CreER(T) to assay temporal activity windows along the proximodistal limb skeleton. Dev Dyn 235, 2603–2612, doi:10.1002/dvdy.20892 (2006). [PubMed: 16894608]
30. Madisen L et al. A robust and high-throughput Cre reporting and characterization system for the whole mouse brain. Nat Neurosci 13, 133–140, doi:10.1038/nn.2467 (2010). [PubMed: 20023653]
31. Voehringer D, Liang HE & Locksley RM Homeostasis and effector function of lymphopenia-induced "memory-like" T cells in constitutively T cell-depleted mice. J Immunol 180, 4742–4753 (2008). [PubMed: 18354198]
32. Snippert HJ et al. Intestinal crypt homeostasis results from neutral competition between symmetrically dividing Lgr5 stem cells. Cell 143, 134–144, doi:10.1016/j.cell.2010.09.016 (2010). [PubMed: 20887898]

33. Shimizu H & Awata T Growth of skeletal bones and their sexual differences in mice. Jikken Dobutsu 33, 69–76 (1984). [PubMed: 6468507]

34. Doucette CR & Rosen CJ Inducible models of bone loss. Curr Protoc Mouse Biol 4, 165–180, doi: 10.1002/9780470942390.mo140071 (2014). [PubMed: 25723184]

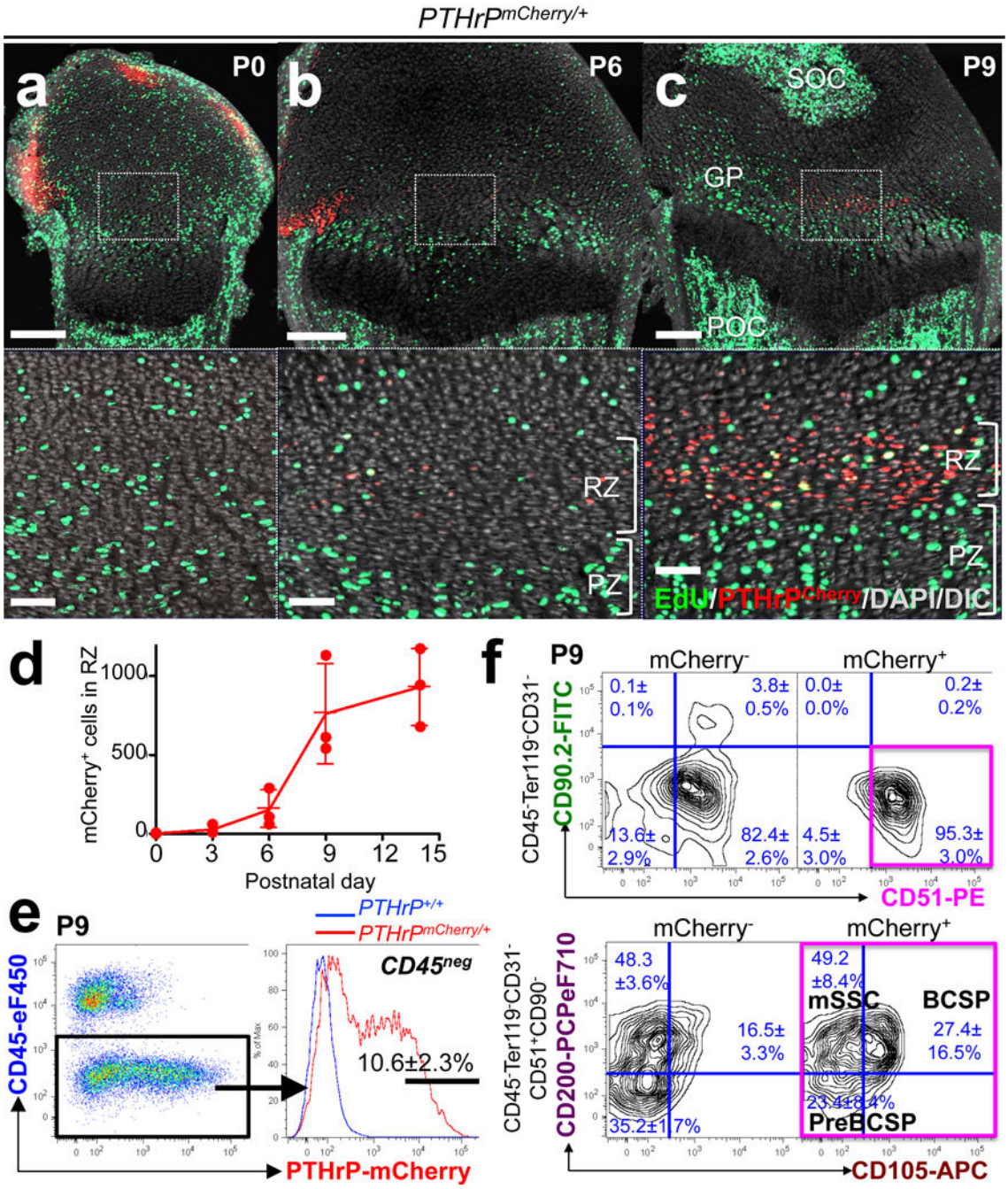

Figure 1. Formation of *PTHrP-mCherry*$^{+}$ chondrocytes in the resting zone of the growth plate.

(a-d) *PTHrP*$^{mCherry/+}$ distal femur growth plates with EdU administration shortly before analysis. Lower panels: magnified views of central growth plates. RZ: resting zone, PZ: proliferating zone, GP: growth plate, POC: primary ossification center, SOC: secondary ossification center. Grey: DAPI and DIC. Scale bars: 200μm (upper panels), 50μm (lower panels). (d): Quantification of mCherry^{+} cells. n=3 mice per group, data are presented as mean ± S.D. **(e)** Flow cytometry analysis of *PTHrP*$^{mCherry/+}$ growth plate cells. n=8 mice, data are presented as mean ± S.D. **(f)** Skeletal stem/progenitor cell surface marker analysis

of *PTHrP*$^{mCherry/+}$ growth plate cells. mCherry^{-}: mCherry^{-} fraction of *PTHrP*$^{mCherry/+}$ cells, mCherry^{+}: mCherry^{+} fraction of *PTHrP*$^{mCherry/+}$ cells. Magenta box: CD45^{-}Ter119^{-}CD31^{-}CD51^{+}CD90^{-}mCherry^{+} fraction. mSSC: mouse skeletal stem cell, BCSP: bone/cartilage/stromal progenitor. n=3 mice per group, data are presented as mean ± S.D.

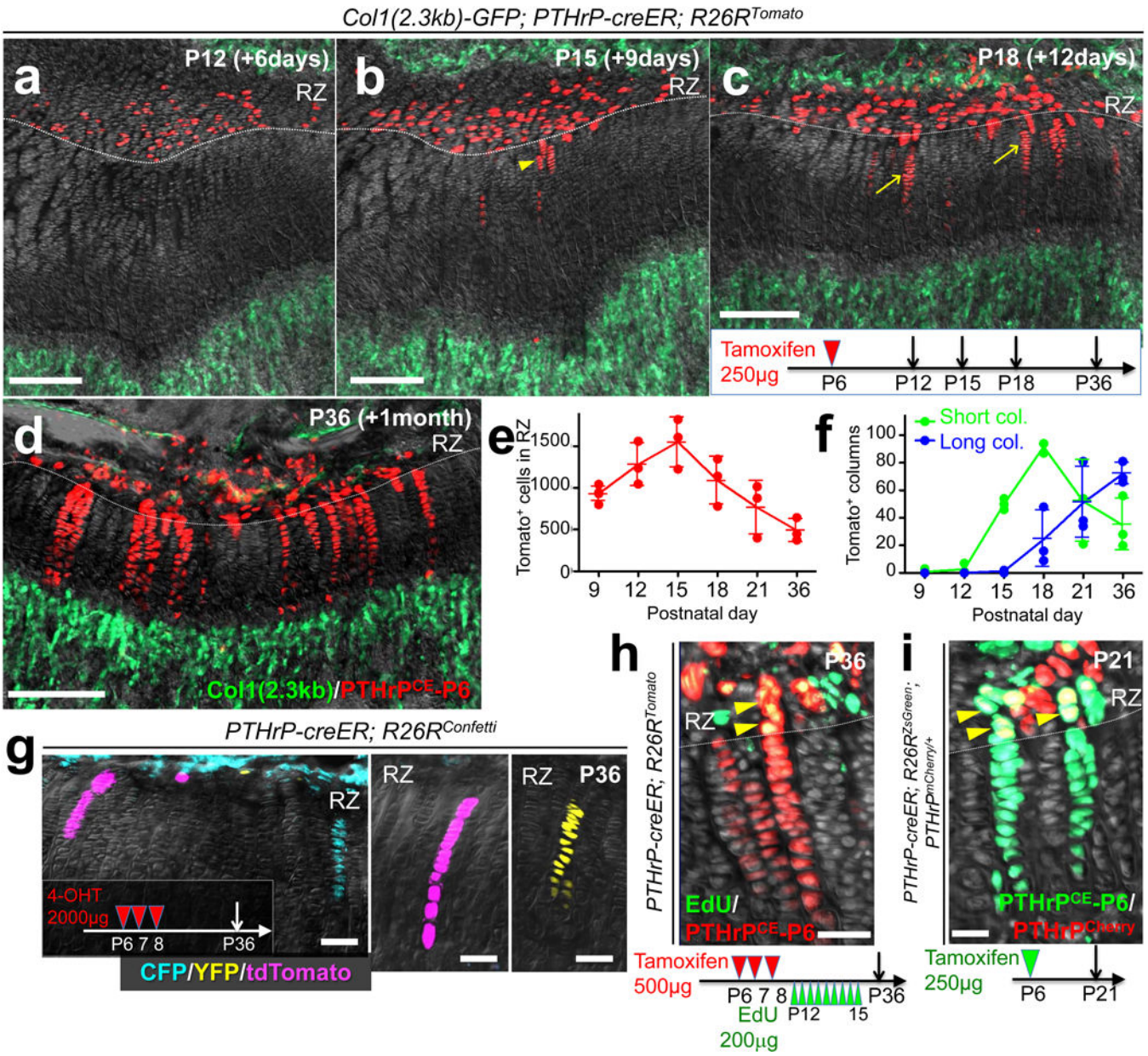

Figure 2. *PTHrP-creER*$^{+}$ resting chondrocytes are the source of columnar chondrocytes.

(a-f) Cell fate analysis of *PTHrP-creER*$^{+}$ resting chondrocytes. *Col1(2.3kb)*-GFP; *PTHrP-creER*; *R26R*$^{\text{Tomato}}$ (P6-pulsed) distal femur growth plates. Arrowhead: short column (<10 cells), arrows: long columns (>10 cells). Scale bars: 200μm. (e,f): Quantification of tdTomato^{+} cells in resting zone (e) (red line) and columns in growth plate (f), short columns (<10 cells, green line) and long columns (>10 cells, blue line). n=5 (P9), n=3 (P12-36) mice per group, data are presented as mean ± S.D. **(g)** *In vivo* clonal analysis of *PTHrP-creER*$^{+}$ resting chondrocytes. *PTHrP-creER; R26R*$^{\text{Confetti}}$ distal femur growth plates (P6/7/8-pulsed). 4-OHT: 4-hydroxytamoxifen. Scale bars: 50μm. n=3 mice. **(h)** EdU label-retention assay of *PTHrP-creER*; *R26R*$^{\text{Tomato}}$ distal femur growth plates (P6/7/8-pulsed). Arrowheads: EdU-retaining tdTomato^{+} cells. Scale bars: 50μm. n=3 mice. **(i)** *PTHrP-*

mCherry expression in *PTHrP-creER*; *R26R*^{ZsGreen}; *PTHrP*$^{mCherry/+}$ distal femur growth plates (P6-pulsed). Arrowheads: *PTHrP*-mCherry^{+}ZsGreen^{+} cells. Scale bars: 20μm. Grey: DAPI and DIC. RZ: resting zone. *n*=3 mice.

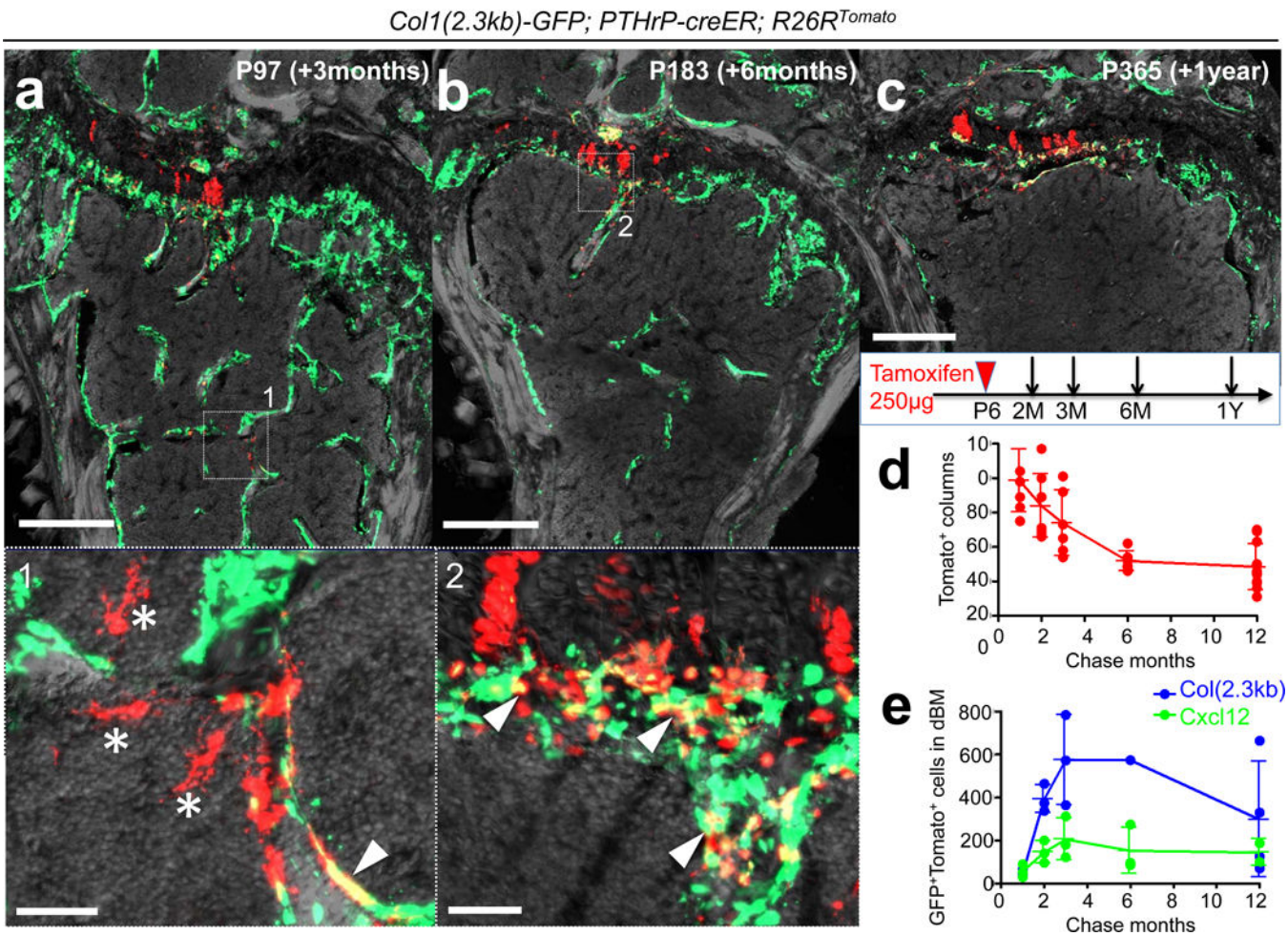

Figure 3. *PTHrP-creER*$^{+}$ resting chondrocytes behave as skeletal stem cells *in vivo*.

(a-c) Long-chase analysis of *PTHrP-creER*$^{+}$ resting chondrocytes. *Col1(2.3kb)*-GFP; *PTHrP-creER*; *R26R*^{Tomato} distal femurs (P6-pulsed). Lower panel: magnified views of marrow space. Arrowheads: *Col1(2.3kb)*-GFP^{+}tdTomato^{+} osteoblasts, asterisks: tdTomato^{+} reticular stromal cells. Grey: DAPI and DIC. Scale bars: 500μm (upper panels), 50μm (lower panels). *n*=3 mice per group, except in (b), *n*=1 mouse. **(d)** Quantification of tdTomato^{+} columns in growth plate (red line) during the chase. *n*=8 (1M, 2M), *n*=6 (3M, 6M), *n*=11 (12M) mice per group, data are presented as mean ± S.D. **(e)** Quantification of *Col1(2.3kb)*-GFP^{+}tdTomato^{+} osteoblasts (blue line) and *Cxcl12*-GFP^{+}tdTomato^{+} stromal cells (green line) in distal bone/bone marrow (dBM: up to 5mm from the growth plate) during the chase. *n*=3 (1M, 2M, 3M for *Col1(2.3kb)*-GFP and *Cxcl12*-GFP, 6M for *Cxcl12*-GFP), *n*=4 (12M for *Col1(2.3kb)*-GFP), *n*=2 (12M for *Cxcl12*-GFP) mice per group, data are presented as mean ± S.D., *n*=1 (6M for *Col1(2.3kb)*-GFP) mouse.

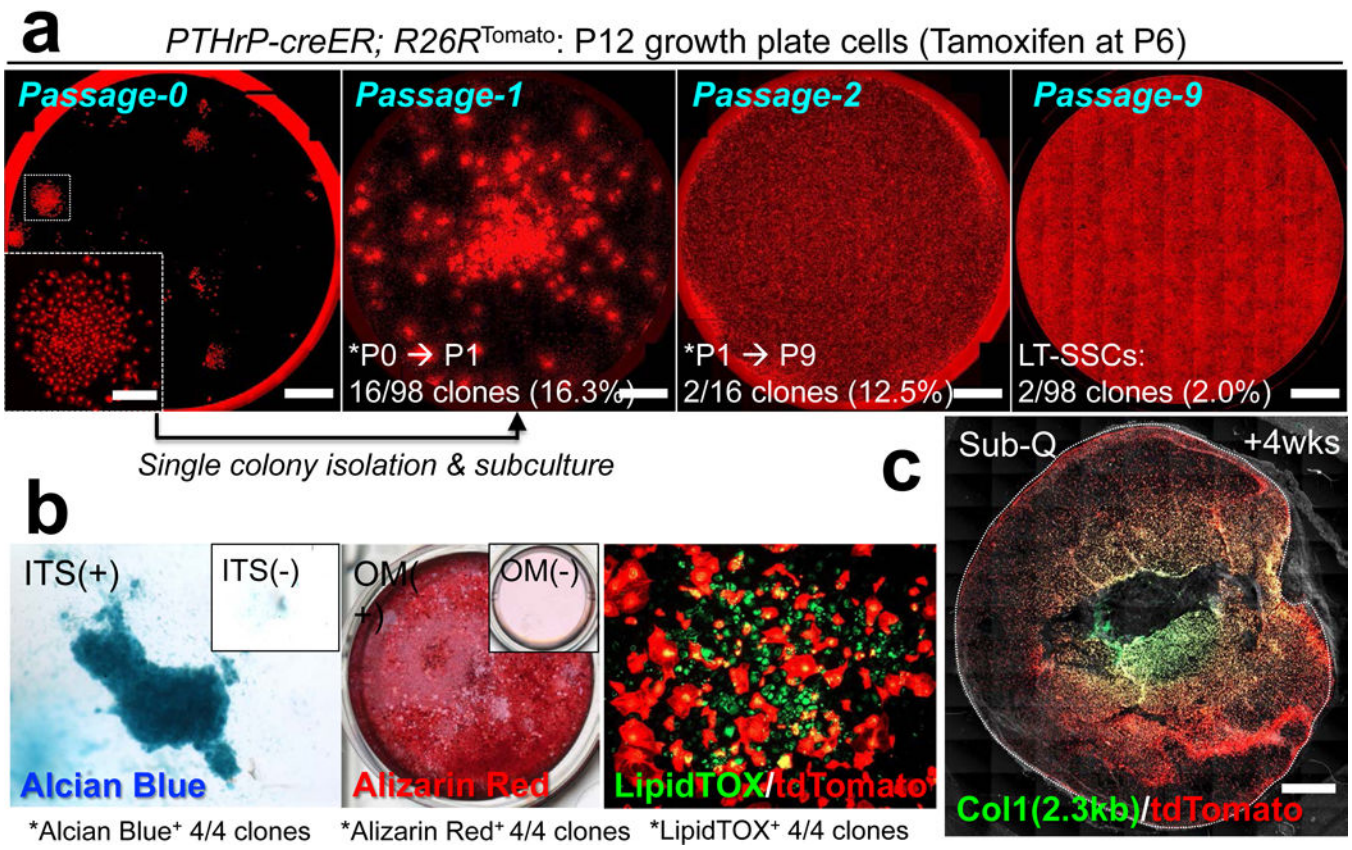

Figure 4. Skeletal stem cell activities of *PTHrP-creER*$^+$ resting chondrocytes *ex vivo*.

(a) Colony-forming assay and subsequent passaging of individual *PTHrP-creER*/tdTomato$^+$ colonies. Inset: magnified view of single colony. Red: tdTomato. Scale bars: 5mm, 1mm (inset). LT-SSCs: long-term skeletal stem cells. n=98 independent experiments. **(b)** Trilineage differentiation of *PTHrP-creER*/tdTomato$^+$ clones (Passage 4~7). Chondrogenic (leftmost), osteogenic (left center) and adipogenic (right center) differentiation conditions. Insets: differentiation medium negative controls. ITS: insulin-transferrin-selenium, OM: osteogenic differentiation medium. Four independent clones were tested. **(c)** Subcutaneous (Sub-Q) transplantation of *PTHrP-creER*/tdTomato$^+$ clones into immunodeficient mice. Dotted line: contour of the plug. Grey: DIC. Scale bars: 1mm. n=8 mice.

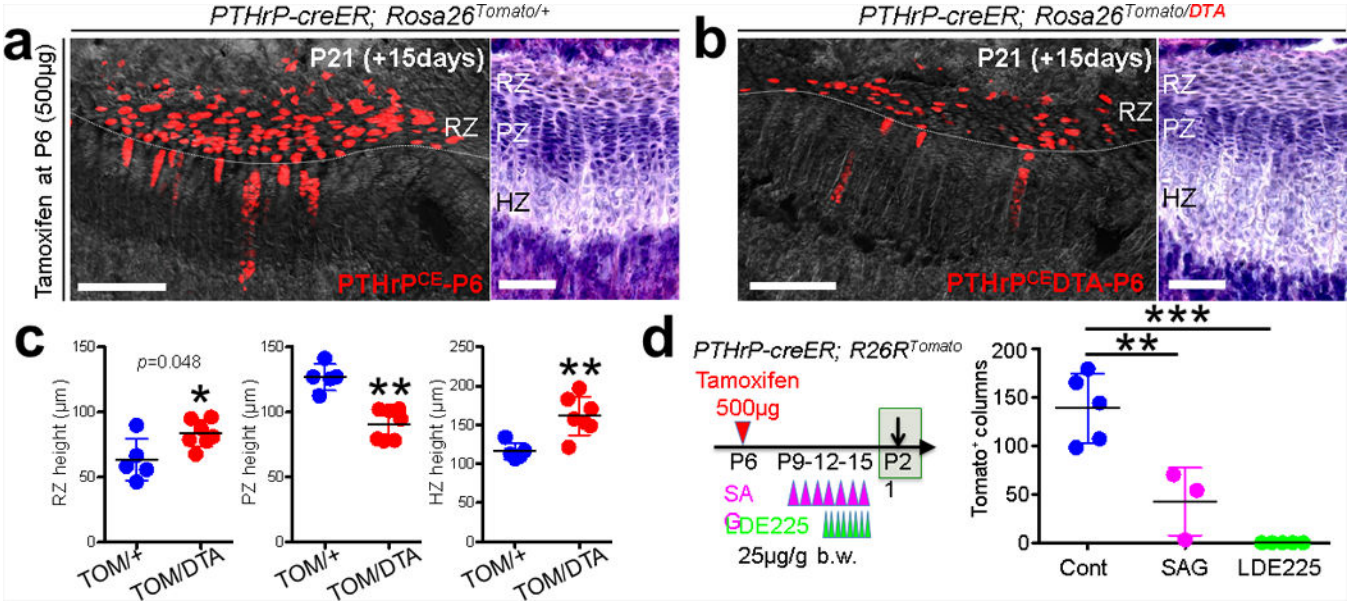

Figure 5. Reciprocal interactions between *PTHrP-creER*$^{+}$ resting chondrocytes and their niche.

(a-c) DTA-mediated ablation of *PTHrP-creER*$^{+}$ resting chondrocytes. (a): *PTHrP-creER*; *Rosa26*$^{lsl\text{-}tdTomato/+}$ (Control), (b): *PTHrP-creER*; *Rosa26*$^{lsl\text{-}Tomato/iDTA}$ (DTA) distal femur growth plates (P6-pulsed). RZ: resting zone, PZ: proliferating zone, HZ: hypertrophic zone. Grey: DAPI and DIC. Right panels: H&E staining. Scale bars: 200μm (left panels) and 100μm (right panels). (c): Quantification of resting (left), proliferating (center) and hypertrophic (right) zone height. TOM: tdTomato. n=5 mice for Control, n=7 mice for DTA, data are presented as mean ± S.D., *p = 0.048, **p = 0.0025 (center), **p = 0.0051 (right), Mann-Whitney's U-test, two-tailed. **(d)** Pharmacological manipulation of Hedgehog signaling. Quantification of tdTomato^{+} columns in *PTHrP-creER*; *R26R*^{Tomato} distal femur growth plates (P6-pulsed). n=5 (Control), n=3 (SAG), n=5 (LDE225) mice per group, data are presented as mean ± S.D., **p < 0.01, ***p < 0.001, Cont vs. SAG: mean diff. = 96.2, 95% confidence interval [41.6, 150.9], Cont vs. LDE225: mean diff. 138.6, 95% confidence interval [91.3, 185.9], SAG vs. LDE225: mean diff. 42.3, 95% confidence interval [−12.3, 97.0], One-way ANOVA followed by Tukey's multiple comparison test. recombination. White boxes: untranslated region (UTR), black boxes: coding region, ex: exon. Blue bars: homology arms, red bars: guide RNAs (gRNAs) as part of CRISP/Cas69 reagents. Red boxes: *Kozak*-mCherry-*bGHpA* cassette replacing the native start codon. Half arrows: primers, wild-type.